

Analysis of the Lorenz Equations for Large r

By A. C. Fowler

In the limit of large r , the Lorenz equations become "almost" conservative. In this limit, one can use the method of averaging (or some equivalent) to obtain a set of two autonomous differential equations for two slowly varying amplitude functions B and D . A stable fixed point of these equations represents the stable periodic solution which is observed at large r . There is an invariant line $B = D$ on which the method breaks down and the averaged equations are no longer valid. In this paper we show how to extend the validity of the analysis by Poincaré-mapping B and D across this line. This extended analysis provides (in principle) a complete recipe for constructing approximate solutions, and shows how a strange invariant set can occur in connection with an essentially analytically constructed two-dimensional mapping.

1. Introduction

The Lorenz equations [10] are a set of three first-order nonlinear differential equations which display chaotic solutions in parts of their parameter ranges. Much that is currently known about these equations is summarized in the book by Sparrow [19]. In particular, it is known that for large values of the bifurcation parameter r , there exists a stable periodic orbit which loses stability as r is decreased via a period-doubling cascade to chaos.

In an effort to understand some of this behavior analytically, a number of different authors have studied the equations asymptotically in the limit $r \rightarrow \infty$. The basic idea stems from Howard [5], and the calculation of the stable limit cycle has been done by Robbins [15, 16] and by Shimizu [17]. Relevant also would be the thesis of Yudovich [20], quoted by Rabinovich [14]. Both Robbins and Shimizu directly calculate the fixed point of the averaged equations one obtains. Poyet [13] considers the evolution equations for the slowly varying amplitude functions, and noted difficulties in certain parts of the averaged phase space. However, it was really Sparrow [19] who explicitly studied these difficulties, and offered a prescription for their resolution and interpretation.

The analysis at high r proceeds by first rescaling the variables, and then carrying out a multiple scale expansion in the parameter $\epsilon = 1/\sqrt{r\sigma} \ll 1$. For $\epsilon = 0$, there are two constants of the motion (B, D), and when $\epsilon \ll 1$, these vary slowly in time. By averaging over a period of the underlying oscillation, one obtains two autonomous differential equations for B and D , the fixed points of which correspond to either fixed points or periodic solutions. Particularly, one can identify a stable fixed point in $B > |D|$ which represents the stable periodic solution at large r .

This would essentially close the analytic exploration, since two-dimensional autonomous systems are completely understood, were it not for the fact that there is a peculiar nonuniqueness associated with the averaged equations. This is due to non-Lipschitzian behavior of the system, which in turn is due to the fact that on the line $B = D$, the underlying fast oscillation of the $\epsilon = 0$ system is homoclinic, i.e., has infinite period. Consequently, the averaging procedure on which the analysis is based is not valid, and the nonuniqueness of the averaged equations betrays this fact. Poyet [13] pointed out the problem, although Baker et al. [1] and Marzec and Spiegel [12] have also associated strange behavior with such an invariant line. Sparrow [19] discussed the problem at some length, and suggested that "anomalous" orbits could migrate along $B = D$ in some predictable (in principle) manner, such that anomalous periodic and aperiodic behavior would exist (though not attracting).

The purpose of this paper is to complete (in some sense) the discussion in Sparrow's book, and to give a recipe by which to determine how far anomalous orbits can evolve up the invariant line. In so doing, we construct a semianalytic two-dimensional Poincaré map, which we suggest will exhibit strange (nonattracting) behavior. In this sense, averaging is a possible technique for studying chaos explicitly. Its use here is somewhat different to that explored by Holmes [3, 4], who was more concerned with nonautonomous systems. However, the ideas explored here will also have application in such systems, as well as in other chaotic, almost conservative oscillators.

2. The averaged equations

In this section we derive the averaged equations for the slowly varying amplitudes B and D . The procedure is well known, and so we give only an outline: see [19] for more detail.

The Lorenz equations are

$$\begin{aligned} \dot{x} &= -\sigma x + \sigma y, \\ \dot{y} &= (r - z)x - y, \\ \dot{z} &= xy - bz, \end{aligned} \quad (2.1)$$

where a dot means differentiation with respect to time T . We rescale by writing

$$\epsilon = \frac{1}{\sqrt{r\sigma}}, \quad x = \frac{\xi}{\epsilon}, \quad y = r\eta, \quad z = r(1-w), \quad T = \epsilon t, \quad (2.2)$$

so (2.1) is ($\dot{\xi} = d\xi/dt$, now)

$$\begin{aligned} \dot{\xi} &= \eta - \epsilon\sigma\xi, \\ \dot{\eta} &= w\xi - \epsilon\eta, \\ \dot{w} &= -\xi\eta + b(1-w). \end{aligned} \quad (2.3)$$

We assume now that $\epsilon \ll 1$, $\sigma, b - 1$, and define

$$B^2 = w^2 + \eta^2, \quad D = w + \frac{1}{2}\xi^2. \quad (2.4)$$

One finds

$$\begin{aligned} B\dot{B} &= \epsilon [bw(1-w) - \eta^2], \\ \dot{D} &= \epsilon [b(1-w) - \sigma\xi^2], \end{aligned} \quad (2.5)$$

and thus B and D evolve on the slow time scale $\tau = \epsilon t$. Over a time scale $t - 1$, B and D can be considered constant, and then the fast oscillation solution of (2.3) [neglecting $O(\epsilon)$] is

$$\begin{aligned} \xi &= \pm \{2B(1+U)\}^{1/2} \text{cn } \psi, \\ \eta &= \mp \{2(1+U)\}^{1/2} B \text{sn } \psi \text{ dn } \psi, \\ w &= +B(1 - 2 \text{dn}^2 \psi) \end{aligned} \quad (2.6)$$

if $-1 < U < 1$, and

$$\begin{aligned} \xi &= \pm \{2B(1+U)\}^{1/2} \text{dn } \psi, \\ \eta &= \mp 2B \left\{ \frac{2}{1+U} \right\}^{1/2} \text{sn } \psi \text{ cn } \psi, \\ w &= B(1 - 2 \text{cn}^2 \psi) \end{aligned} \quad (2.7)$$

if $U > 1$, where

$$\begin{aligned} U &= D/B, \quad \psi = \sqrt{B}t + \text{phase}, \\ k^2 &= \begin{cases} (1+U)/2, & U < 1, \\ 2/(1+U), & U \geq 1, \end{cases} \end{aligned} \quad (2.8)$$

and k is the modulus of the elliptic functions sn, cn, dn. By integrating over

$P = 2K(k)/\sqrt{B}$, where K is the complete elliptic integral of the first kind (equal to the period for $U > 1$, half the period for $U < 1$), we find

$$B(t+P) - B(t) \approx \epsilon P [bc - \frac{1}{3}(b+2)B + \frac{2}{3}(1-b)cD], \quad (2.9)$$

$$D(t+P) - D(t) \approx \epsilon P [b(1-cB) - 2\sigma(D-cB)],$$

where

$$c = -u_3 - (u_1 - u_3)E/K, \quad (2.10)$$

and $u_1 > u_2 > u_3$ are the roots of $(U+u)(1-u^2) = 0$. The averaged differential equations for $B(\tau)$, $D(\tau)$, $\tau = \epsilon t$, follow from identifying $[B(t+P) - B(t)]/\epsilon P \approx B'(\tau)$, and similarly for D :

$$B' \approx f(B, D), \quad (2.11)$$

$$D' \approx g(B, D),$$

where f and g are the expressions in square brackets in (2.9). The procedure is invalid when the right-hand sides of (2.9) are no longer small, which is when $P \sim 1/\epsilon$: i.e. $K \sim 1/\epsilon$. As $K \rightarrow \infty$ in (2.11) we find that the limiting forms of the equations can be written

$$B' = b(1-B) - \frac{4}{\ln(1/|\Sigma|)} \left\{ b + \frac{2}{3}(1-b)B \right\} + O(\Sigma), \quad (2.12)$$

$$\Sigma' \ln(1/|\Sigma|) = -\frac{\mu}{24} + O(\Sigma \ln(1/|\Sigma|)),$$

where

$$\mu = 6\sigma - b - 2 - \frac{3b}{B}, \quad (2.13)$$

and

$$D = B(1 + 32\Sigma). \quad (2.14)$$

According to (2.12), Σ reaches zero in finite time, that is, trajectories obeying (2.11) reach the invariant line $\Sigma = 0$ in finite τ . Since $K \sim \frac{1}{2} \ln(1/|\Sigma|)$, (2.12) is invalid when $|\Sigma| = \exp(-O(1/\epsilon))$, i.e. is exponentially small. The problem is thus to find a way to "continue" B and D across, or along, $B = D$.

3. Poincaré maps near the invariant line

The expansions (2.6), (2.7), e.g.

$$w = B(\tau) [1 - 2\text{dn}^2(\sqrt{B}\tau + \theta(\tau))] + O(\epsilon), \quad (3.1)$$

can be thought of as a multiple scale approximation. A more elegant method of obtaining higher-order terms is that due to Kuzmak [8], extended by Luke [11], and by Kogelman and Keller [7] and Kevorkian and Cole [6]. In this method the fast time t^* is chosen to satisfy $dt^*/dt = \phi(\tau)$, where ϕ is chosen to keep the period P of the fast oscillation constant: in our case we would have $\phi \propto \sqrt{B}/K$. However: (1) this method also breaks down when $\phi \rightarrow 0$, i.e. $K \rightarrow \infty$; (2) at leading order, it is equivalent to the results previously obtained by averaging. We therefore do not discuss it further. It has been used in the present context by Poyet [13]; see also Shimizu and Ichimura [18].

The key to extending the analysis to the case $B - D \approx 0$ is to realize that the derivation in Section 2 actually produces a Poincaré map (2.9), which is *then* approximated by a differential equation. Thus, we choose to think of (2.9) in terms of differential equations only when $B - D = O(1)$, for the purpose of using a phase-plane analysis. Thus, as $\Sigma \rightarrow 0$, given by (2.14), we have $P \sim \ln(1/|\Sigma|)$, and the limiting form of (2.9) is, by inspection of (2.12),

$$B(t+P) - B(t) \approx \frac{\epsilon}{\sqrt{B}} \left[b(1-B) \ln \frac{1}{|\Sigma|} - 4 \left\{ b + \frac{2}{3}(1-b)B \right\} + O \left(\Sigma \ln \frac{1}{|\Sigma|} \right) \right], \quad (3.2)$$

$$\Sigma(t+P) - \Sigma(t) \approx \frac{\epsilon}{\sqrt{B}} \left[-\frac{\mu}{24} + O(\Sigma) \right],$$

where the right-hand sides are evaluated at t .

That (3.2) and (2.9) are Poincaré maps follows because the integration is over a period of w ; for example, we could choose as return plane any surface $w = \text{constant}$. We will in fact choose the return plane to be $w = 0$, close to $z = r - 1$, a common choice [19].

When Σ is small, the fast oscillation is close to a homoclinic orbit

$$w \approx B[1 - 2\text{sech}^2\sqrt{B}t], \quad (3.3)$$

and one should really calculate the first return map in this case by writing

$$w = w_0 + \epsilon W, \quad (3.4)$$

where w_0 is given by (3.3) (similarly for ξ and η), and directly calculating the values of B and Σ when the trajectory next intersects $w = 0$. We would want the calculated map to match to (3.2) as Σ becomes large, but since (3.2) is return-surface independent, we cannot expect it to be identical. The calculation is straightforward but a little lengthy, and details are omitted here (see [16] for a similar calculation). One finds that (3.2) is reproduced, except that $\ln(1/|\Sigma|)$ in (3.2)₁ is replaced by $\ln(1/|\Sigma - \epsilon\nu|)$, where

$$\nu = \frac{(\sqrt{2}-1)\mu + b - 1}{48\sqrt{2}B}. \quad (3.5)$$

This matches, as required, to (3.2). The meaning of the alteration is just that $\Sigma = \epsilon\nu$ is on the stable manifold of the origin at $w = 0$. Obviously, ν depends on the location of the return plane.

Importantly, note that successive iterates Σ_n of Σ do not approach the invariant line $\Sigma = 0$, but simply pass through, unless $\Sigma_n - \epsilon\nu = \exp\{-O(1/\epsilon)\}$ for some iterate [as we shall see, the derivation of (3.2) incorporating (3.5) is invalid then]. That is, except for this special case, the continuation of B and D through $B = D$ is direct—no migration up the line occurs.

The interesting case is thus when $\Sigma_N - \epsilon\nu = \exp\{-O(1/\epsilon)\}$ for some N . We wish to find what the appropriate return map in this case is. The idea now is that the orbit is exponentially close to the stable manifold of the origin. Therefore it spends a long time ($t - 1/\epsilon$) in the neighborhood of the origin, and the trajectory itself involves two time scales; behavior on each must be matched to find the mapping. The procedure is very close to that used in studying homoclinic bifurcations for the case of a maximally unstable real eigenvalue and a minimally unstable real eigenvalue, as in the Lorenz system [19].

Consider an orbit with "initial" values

$$w = \epsilon W_0, \quad \xi = \sqrt{2B_0} + \epsilon X_0, \quad \eta = -B_0 + \epsilon Y_0, \quad (3.6)$$

when $t = t_0 = [\operatorname{sech}^{-1}(1/\sqrt{2})]/\sqrt{B_0}$. This orbit lies close to the homoclinic orbit

$$\begin{aligned} \xi_0 &= 2\sqrt{B_0} \operatorname{sech}\sqrt{B_0} t \\ \eta_0 &= -2B_0 \operatorname{sech}\sqrt{B_0} t \tanh\sqrt{B_0} t, \\ w_0 &= B_0(1 - 2 \operatorname{sech}^2\sqrt{B_0} t). \end{aligned} \quad (3.7)$$

Therefore we put

$$\begin{aligned} \xi &= \xi_0 + \epsilon X + \dots, \\ \eta &= \eta_0 + \epsilon Y + \dots, \\ w &= w_0 + \epsilon W + \dots \end{aligned} \quad (3.8)$$

into the equations, and find

$$\begin{aligned} \dot{X} &= Y - \sigma\xi_0, \\ \dot{Y} &= w_0 X + \xi_0 W - \eta_0, \\ \dot{W} &= -\eta_0 X - \xi_0 Y + b(1 - w_0), \end{aligned} \quad (3.9)$$

to leading order. Notice that

$$\begin{aligned} B^2 &= B_0^2 + 2\epsilon[w_0 W + \eta_0 Y] + \dots, \\ D &= B_0 + \epsilon[W + \xi_0 X] + \dots, \end{aligned} \quad (3.10)$$

and that

$$[w_0 W + \eta_0 Y]' = bw_0(1 - w_0) - \eta_0^2 = \dot{Q}, \quad (3.11)$$

say, and

$$[W + \xi_0 X]' = b(1 - w_0) - \sigma\xi_0^2 = \dot{P}, \quad (3.12)$$

say. Using (3.7), we obtain

$$\begin{aligned} P &= bB_0(1 - B_0)t - 2b\sqrt{B_0} \tanh\sqrt{B_0} t + \frac{1}{3}(b - 1)B_0^{3/2} \tanh^3\sqrt{B_0} t, \\ Q &= b(1 - B_0)t - 2(2\sigma - b)\sqrt{B_0} \tanh\sqrt{B_0} t, \end{aligned} \quad (3.13)$$

and defining

$$T_0 = \operatorname{sech}^{-1}(1/\sqrt{2}), \quad (3.14)$$

then $P = P_0$, $Q = Q_0$ when $t = t_0$, where

$$\begin{aligned} P_0 &= b\sqrt{B_0}(1 - B_0)T_0 - b\sqrt{2B_0} + \frac{1}{3}(b - 1)(2B_0)^{3/2}, \\ Q_0 &= \frac{b(1 - B_0)T_0}{\sqrt{B_0}} - (2\sigma - b)\sqrt{2B_0}. \end{aligned} \quad (3.15)$$

Thus, (3.11) and (3.12) give

$$\begin{aligned} w_0 W + \eta_0 Y &= Q - Q_0 - B_0 Y_0, \\ W + \xi_0 X &= P - P_0 + \sqrt{2B_0} X_0 + W_0. \end{aligned} \quad (3.16)$$

One can now eliminate W and Y and solve for X by quadrature. The result is

$$\begin{aligned} X &= \frac{\operatorname{sech}\sqrt{B_0} t \tanh\sqrt{B_0} t}{2B_0} \\ &\times \left[4B_0 X_0 - R_0 + \left(\frac{1}{2}A_0 + A_1\right)t - \frac{1}{2}A_2 t^2 \right. \\ &\quad + \frac{A_2}{\sqrt{B_0}} t \cosh\sqrt{B_0} t - \frac{A_0 + A_1}{\sqrt{B_0}} \coth\sqrt{B_0} t \\ &\quad + \frac{A_0}{2\sqrt{B_0}} \sinh\sqrt{B_0} t \cosh\sqrt{B_0} t + \frac{A_3 - A_4}{2\sqrt{B_0}} \sinh^2\sqrt{B_0} t \\ &\quad \left. - 2\sigma \operatorname{sech}\sqrt{B_0} t \tanh\sqrt{B_0} t \ln|\sinh\sqrt{B_0} t| \right], \end{aligned} \quad (3.17)$$

where R_0 is the constant such that $X = X_0$ when $t = t_0$, and

$$\begin{aligned} A_0 &= P_0 + B_0 Y_0 - B_0 [Q_0 - \sqrt{2B_0} X_0] - W_0, \\ A_1 &= 2B_0 [Q_0 - \sqrt{2B_0} X_0], \\ A_2 &= 2bB_0(1 - B_0), \\ A_3 &= 2b\sqrt{B_0} + 2B_0^{3/2}(2\sigma - b), \\ A_4 &= 4B_0^{3/2}(2\sigma - b) + \frac{1}{2}(b - 1)B_0^{3/2}. \end{aligned} \tag{3.18}$$

The important result is that, after some simplification, one finds

$$X - C_{\pm} e^{\pm\sqrt{B_0}t} \quad \text{as } t \rightarrow \pm\infty, \tag{3.19}$$

where

$$\begin{aligned} C_{\pm} &= \pm C_0 - \frac{\mu}{12}, \\ C_0 &= \frac{A_0}{8B_0^{3/2}}, \end{aligned} \tag{3.20}$$

and μ is given by (2.13). A_0 is related to the initial values X_0, Y_0, W_0 , and to

$$P_0 - B_0 Q_0 = +\frac{1}{2}\sqrt{2} B_0^{3/2} \left[6\sigma - 2b - 1 - \frac{3b}{B_0} \right]. \tag{3.21}$$

Thus as $t \rightarrow \infty$

$$\xi \sim 4\sqrt{B_0} e^{-\sqrt{B_0}t} + \epsilon C_+ e^{\sqrt{B_0}t}, \tag{3.22}$$

and the ordering of the expansion breaks down when t is large $\{ \sim \ln(1/\epsilon|C_+|) \}$.

If $C_+ = O(1)$, then the trajectory only spends a time $\sim \ln(1/\epsilon)$ near the origin, so it does not change significantly, and no further solution is necessary (at least at leading order). One simply matches (3.22) to a (phase-shifted) near-homoclinic orbit on the other side:

$$\xi \sim 4\sqrt{B_0} e^{\sqrt{B_0}t'} + \epsilon C'_- e^{-\sqrt{B_0}t'}, \tag{3.23}$$

and the constants $t' - t$ and C'_- (value of C_- for the next passage through $w = 0$) are chosen to equate (3.22) and (3.23). In this way we obtain (3.2). In the case

$C_+ = \exp[-O(1/\epsilon)]$, the trajectory will spend a time $O(1/\epsilon)$ near the origin, w changes significantly, and a separate calculation is necessary.

Define $\tau = \epsilon t$ (perhaps plus a constant), and

$$C_+ = \pm e^{-R/\epsilon}, \quad R = O(1). \tag{3.24}$$

For $\tau = O(1)$; the leading-order equations for ξ, η , and w are

$$\dot{\xi} = \eta, \quad \dot{\eta} = w\xi, \quad w' = b(1 - w), \tag{3.25}$$

where we use the fact that in the region of interest, ξ and η will be exponentially small. Here $w' = dw/d\tau, \xi = d\xi/dt$, etc. Thus $w = w(\tau)$, in fact,

$$w = 1 - (1 - B_0)e^{-\tau}. \tag{3.26}$$

where $\tau = 0$ marks the beginning of this slow phase. Asymptotic solutions of (3.25)_{1,2} are then, to leading order,

$$\xi \sim G_1(\tau) \exp\left[\frac{\lambda_+(\tau)}{\epsilon}\right] + G_2(\tau) \exp\left[\frac{\lambda_-(\tau)}{\epsilon}\right], \tag{3.27}$$

where

$$\lambda_{\pm} = \pm \int_0^{\tau} [1 - (1 - B_0)e^{-\tau}]^{1/2} d\tau, \tag{3.28}$$

and matching to (3.22) requires

$$\begin{aligned} G_1(\tau) &= \epsilon C_n^+ g_1(\tau), \quad g_1(0) = 1, \\ G_2(\tau) &= 4\sqrt{B_0} g_2(\tau), \quad g_2(0) = 1. \end{aligned} \tag{3.29}$$

Matching to the next (near-homoclinic) pulse uses (3.23), but with B_0 replaced by its value at $\tau = \tau^*$, where τ^* is the value at which the trajectory "emerges" from the origin ($\tau = \tau^* + \epsilon t'$):

$$B_1 = 1 - (1 - B_0)e^{-\tau^*}, \tag{3.30}$$

$$\epsilon C_n^+ g_1(\tau^*) \exp\left[\frac{\lambda_+(\tau^*)}{\epsilon}\right] = 4\sqrt{B_1}, \tag{3.31}$$

$$4\sqrt{B_0} g_2(\tau^*) \exp\left[-\frac{|\lambda_-(\tau^*)|}{\epsilon}\right] = \epsilon C'_-. \tag{3.32}$$

For given C_n^+, B_0 , (3.30)–(3.32) define the values of B_1, τ^* , and C'_- . The functions g_1 and g_2 are not determined at this order [they correspond to higher-order terms in a WKB expansion of (3.25)], but they are not necessary. At leading order, these relations give, with (3.24),

$$R = \int_0^{\tau^*} [1 - (1 - B_0)e^{-\tau}]^{1/2} d\tau, \tag{3.33}$$

which defines τ^* , and

$$C'_- = 0. \tag{3.34}$$

It remains to relate C_\pm to X_0, Y_0, Z_0 and hence to successive values of B and D . Evidently we can choose $Y_0 = W_0 = 0$ on each passage, thus defining

$$B_n = B_0, \quad D_n = B_n(1 + 32\Sigma_n) = B_n + \epsilon\sqrt{2B_n}X_0; \tag{3.35}$$

then using (3.20) and (3.21), we find

$$C_0 = 4\sqrt{B_n} \left[\Sigma_n + \frac{\epsilon(\mu - b + 1)}{48\sqrt{2B_n}} \right], \tag{3.36}$$

whence

$$C_+ = \frac{4}{\epsilon}\sqrt{B_n}[\Sigma_n - \epsilon\nu(B_n)], \tag{3.37}$$

where ν is given by (3.5), and

$$C'_- = \frac{4}{\epsilon}\sqrt{B_{n+1}}[\Sigma_{n+1} + \epsilon\omega(B_{n+1})], \tag{3.38}$$

where

$$\omega(B_{n+1}) = \frac{(\sqrt{2} + 1)\mu - b + 1}{48\sqrt{2B_{n+1}}}, \tag{3.39}$$

$\mu(B_{n+1})$ being given by (2.13). On the plane $w=0$, $\Sigma = \epsilon\nu$ is on the stable manifold of the origin, and $\Sigma = -\epsilon\omega$ is on the unstable manifold. Thus a precisely homoclinic orbit (of simplest form) requires $\omega(B_{n+1}) + \nu(B_{n+1}) = 0$, that is, $\mu = 0$.

To order ϵ , the first return map for B_n is just

$$B_{n+1} = 1 - (1 - B_n)e^{-\tau^*}, \tag{3.40}$$

where τ^* is defined by (3.33), (3.24), and (3.37), and

$$\int_0^{\tau^*} [1 - (1 - B_n)e^{-\tau}]^{1/2} d\tau = \epsilon \ln \left[\frac{\epsilon}{4\sqrt{B_n}|\Sigma_n - \epsilon\nu(B_n)|} \right]; \tag{3.41}$$

the value of Σ_{n+1} is then just

$$\Sigma_{n+1} \approx -\epsilon\omega(B_{n+1}). \tag{3.42}$$

(3.40) and (3.42) define the Poincaré map [to $O(\epsilon)$] valid for $|\Sigma_n - \epsilon\nu(B_n)| \ll 1$ [specifically $\exp\{-O(1/\epsilon)\}$].

As well as (3.7), there is a homoclinic orbit $(-\xi_0, -\eta_0, w_0)$, due to the symmetry of the equations. However, since B and D are invariant under this symmetry, it follows that the analysis above is also. Hence we have obtained a map valid for both cases. Notice that as $|\Sigma_n - \epsilon\nu|$ increases, $B_{n+1} = B_n + O(\epsilon)$, and then $\Sigma_{n+1} - \Sigma_n \approx -\epsilon[\nu(B_n) + \omega(B_{n+1})] \approx -\epsilon[\nu(B_n) + \omega(B_n)] = -\epsilon\mu/24\sqrt{B_n}$, from (3.5) and (3.39), which matches to (3.2) [as does (3.40) ($\tau^* \rightarrow 0$)].

4. A reduced mapping

At this point we have a Poincaré map in two pieces, which is not particularly susceptible to any kind of analysis, although we can to some extent validate the qualitative discussion in [19, p. 140 f.]. To go further, it is useful to take advantage of what is known about the phase plane of (2.11); the relevant information is indicated in Figure 1. For $b < b^* \in (2, 2.67)$, numerical solution of (2.11) indicates that the averaged trajectory from O ($B = D = 1$) loops round and hits the

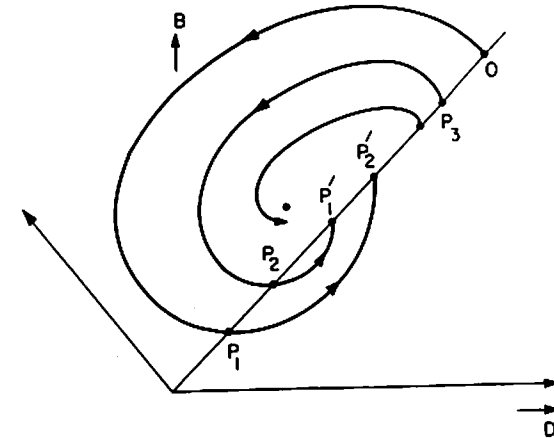


Figure 1. Phase plane of (B, D) for sufficiently small b . Trajectories leaving $B = D$ in P_3O return to $B = D$ in P_1P_2 , and thence to $P_1'P_2'$.

invariant line, as shown. For $\mu > 0$, (nonanomalous) trajectories near $\Sigma = 0$ cross in the direction of decreasing Σ (decreasing $D - B$), and vice versa. We are interested in those orbits which leave the invariant line and return there. For these, we can define a return map on the subset of the (B, D) plane $\Gamma: B \in P_1 P_2 \cup P_3 O, \Sigma$ between $-\epsilon\omega(B)$ and $\epsilon\nu(B)$, where P_1 is the point in the invariant line for which the trajectory out from O returns to $D = B$. (Note that the tenor of this analysis will be applicable to other systems, where strange *attractors* may exist [18, 12, 1].)

The line segment ABC (excluding anomalous points near A) in Figure 2 maps, after an integral number (N) of iterations, to some line segment $A'B'C'$ which cuts across Γ as shown. The relative extension of $A'B'C'$ on the next iteration is $O(\epsilon)$, since the B -values at A' and C' are $O(\epsilon)$ apart, and using (3.2), we see that at the $(n + 1)$ th iteration, A' effectively maps to $A'' = C'$. We know points near (not too near) B' map to points near B'' . Therefore, the segment ABC is taken into the segment $B'C'(A'')B'$, excluding anomalous points near A and near B , which we will put in in a moment. Apart from the anomalous points, the nonintersection of orbits in $\Sigma \neq 0$ implies that the B -values in $P_3 O$ get mapped to $P_2 P_1$ in monotonic fashion; likewise $P_1 P_2$ gets mapped to $P_2' P_1'$ monotonically. This gives a function $f(B)$, which is shown in Figure 3, where we have indicated $P_2' \notin P_3 O$, which seems appropriate to the Lorenz system (e.g. at $b = 1, \sigma = 10$). Other systems might have $P_1' P_2' \subset P_3 O$ (e.g. perhaps [1]).

Now we can define

$$N = \frac{1}{\epsilon} \oint \frac{d\tau}{P(B, D)}, \tag{4.1}$$

where the integral is taken along an (averaged) trajectory. Since P is the (local) period, N is the number of iterations of the Poincaré map between the endpoints

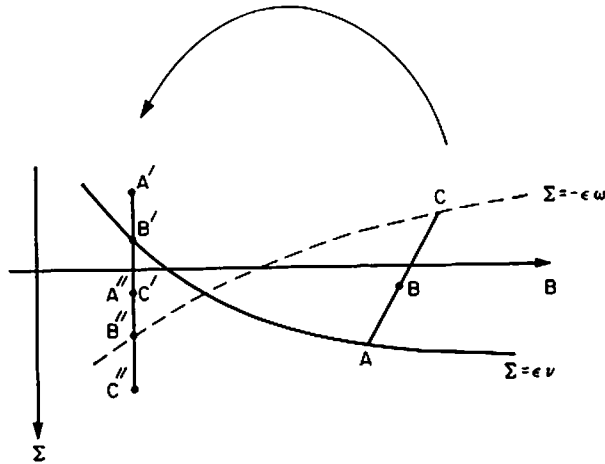


Figure 2. After M iterates, for some integer M , ABC is mapped to $A'B'C'$, and thence to $A''B''C''$.

of the integral. If we define $N(\bar{B})$ as

$$N = \frac{1}{\epsilon} \int_C^{B''} \frac{d\tau}{P} \tag{4.2}$$

along a trajectory, where (as shown in Figure 2) \bar{B} is the value of B at C (on $\Sigma = -\epsilon\omega$) and B'' is the point where that trajectory (excluding anomalous behavior) next hits $\Sigma = -\epsilon\omega$. As Σ increases, the "period" $P = 2K$ decreases monotonically, and it is reasonable to suppose that therefore N increases monotonically with \bar{B} in $P_3 O$ (and decreases in $P_1 P_2$). There will be $O(1/\epsilon)$ values of \bar{B} [spaced $O(\epsilon)$ apart] for which N is exactly an integer. For noninteger values, we can interpolate linearly between the next lower and the next higher integer value to find just where C' in Figure 2 is. It is clear that if we parametrize the Σ range of Γ by $\theta \in (0, 2\pi]$ (include C but not A), i.e.

$$\Sigma = \epsilon\nu - \epsilon(\nu + \omega)\theta/2\pi, \tag{4.3}$$

then the relation between successive (nonanomalous) values of Σ in Γ is locally equivalent to a rotation [which depends on the B -value at C in Figure 2 via (4.2)]: as shown in Figure 4, if B_1, B_2 are two successive values [$B_2 - B_1 = O(\epsilon)$] for which N in (4.2) is integral, then if B [$\in (B_1, B_2)$] labels an arc MN in Γ ($\theta \in (0, 2\pi]$), then its endpoint N' on the $N(B_1)$ th iterate has a θ -coordinate given by

$$\theta \approx \left[\frac{B - B_1}{B_2 - B_1} \right] 2\pi. \tag{4.4}$$

If we denote

$$\epsilon N(\bar{B}) = \phi(\bar{B}), \tag{4.5}$$

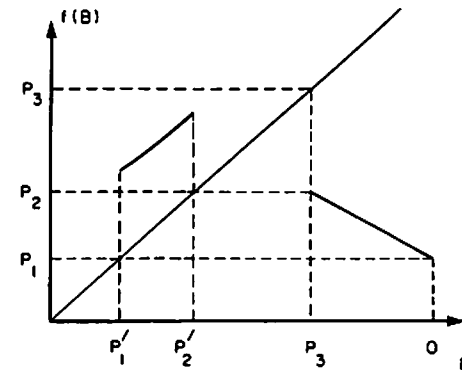


Figure 3. The mapping $f(B)$ (schematic).

put $B_1 = \bar{B}$, and Taylor-expand $\phi(B_2)$ about \bar{B} , then (4.4) is to $O(\epsilon)$

$$\begin{aligned} \frac{\theta}{2\pi} &\approx \frac{(B - \bar{B})\phi'(\bar{B})}{\epsilon} \\ &\approx N(B) - N(\bar{B}) \\ &= N(B) - [N(B)], \end{aligned} \tag{4.6}$$

where $[x]$ is the integer next lower than x . This gives the θ -value of N' . For any $\theta \in (0, 2\pi]$ at B (MN), the corresponding value of θ , say θ' at $f(B)$ (see Figure 3) is

$$\frac{\theta'}{2\pi} = \frac{\theta}{2\pi} - \{1 - (N(B) - [N(B)])\} \text{ mod } 1, \tag{4.7}$$

or

$$\theta' = \theta + 2\pi\{N(B) - [N(B)]\} \text{ mod } 2\pi. \tag{4.8}$$

simply a rotation on the unit circle.

At this point the map is of the form (4.8), together with

$$B' = f(B) \tag{4.9}$$

(see Figure 3), but excluding anomalous points.

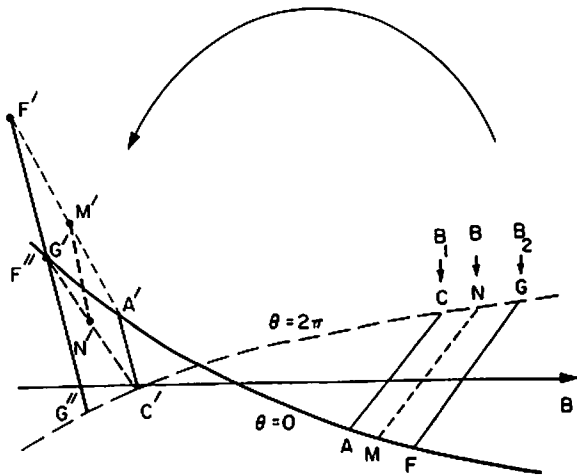


Figure 4. AC and FG are mapped after $N(B_1)$ and $N(B_2) = N(B_1) + 1$ iterations exactly into $A'C'$ and $F'G'$, respectively. MN and its image $M'N'$ are linearly interpolated between them.

To consider these, we focus on points (B_n, θ_n) near A in Figure 2, i.e. for which $|\theta_n|$ is exponentially small. Thus (4.3) and (3.4) define τ^* as

$$\int_0^{\tau^*} [1 - (1 - B_n)e^{-\tau}]^{1/2} d\tau = \epsilon \ln \left[\frac{12\pi}{\mu|\theta_n|} \right]. \tag{4.10}$$

and the next iterates are given by (3.40) and (3.42):

$$B_{n+1} = 1 - (1 - B_n)e^{-\tau^*}, \tag{4.11}$$

$$\theta_{n+1} = 2\pi.$$

(4.10) can be written

$$e^{-\tau^*} = g(|\theta_n|'; B_n), \tag{4.12}$$

where

$$g(1) = 1, \quad g'(0) < 1, \tag{4.13}$$

$$g'(1) = 1/\sqrt{B}.$$

as shown in Figure 5. [We put $(\mu/12\pi)' \approx 1$.] Then the anomalous mapping is of the form, for $\theta + 2\pi\{N(B) - [N(B)]\}$ exponentially small,

$$\theta' = 2\pi,$$

$$B' = 1 - [1 - f(B)] g[|\theta + 2\pi\{N(B) - [N(B)]\}'|; B]. \tag{4.14}$$

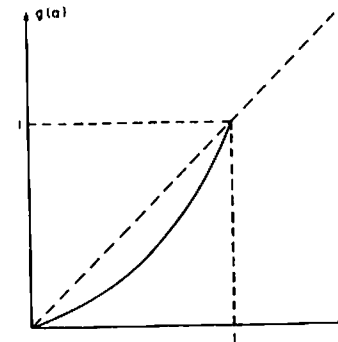


Figure 5. The function $g(\alpha)$ (schematic).

It is clear that (4.14) matches continuously to (4.8) and (4.9). Therefore a uniformly valid Poincaré map on Γ , as parametrized by B and θ , is

$$\begin{aligned} B' &= 1 - [1 - f(B)] g[|\theta + 2\pi(N(B) - [N(B)])|'; B], \\ \theta' &= \theta + 2\pi(N(B) - [N(B)]) \text{ mod } 2\pi. \end{aligned} \tag{4.15}$$

The choice of a reduced set Γ for the map is similar to the set used by Levi [9] and Grasman et al. [2] in studying analytic maps for the forced Van der Pol oscillator. Finally note that (4.15) is simply written

$$\begin{aligned} \theta' &= \theta + 2\pi N(B) \text{ mod } 2\pi, \\ B' &= 1 - [1 - f(B)] g(|\theta'|'; B). \end{aligned} \tag{4.16}$$

We will denote this map as Λ .

5. Discussion

It is not our purpose to give substantive numerical analysis of the map Λ (4.16)—in particular, because there is no attracting behavior. This is intuitively seen by examining Figure 1 (or Figure 3): “most” points on the cylinder $0 < B \leq 1, 0 < \theta \leq 2\pi$ are mapped from P_3O to P_1P_2 , and from P_1P_2 to the fixed point in $D < B$. We are interested in whether (4.16) has an associated invariant set of points which are repeatedly mapped from P_1P_2 to P_3O to P_1P_2 to The points which map from P_1P_2 to P_3O are those sufficiently close to the spiral $\theta + 2\pi N(B) = 0$, which twists round $O(1/\epsilon)$ times in $P_1P_2 \times (0, 2\pi] = C_1$, say. Consider a δ -neighborhood of this spiral in C_1 , where δ is $\exp[-O(1/\epsilon)]$ and depends on B in such a way that the boundaries $|\theta + 2\pi N(B)| = \delta$ of this spiral ribbon S_1 are mapped under (4.16) to P_3 . Since $\theta + 2\pi N(B) = 0$ is mapped to $B = 1$, each line segment of the ribbon S_1 , $B = \text{constant}$ is mapped to a folded line segment which goes from P_3 to O and back to P_3 (not along quite the same path). Consequently, the spiral ribbon S_1 is mapped to a folded (essentially straight) ribbon S'_1 in $C_2 = P_3O \times (0, 2\pi]$. See Figure 6. Note the large extension and contraction of S_1 .

Now the mapping Λ from C_2 to C_1 takes this very thin ribbon S'_1 , and winds it up as a spiral ribbon (different to S_1) about the cylinder C_1 . There will be $O(1/\epsilon)$ pairs of points of intersection (pairs because of the folding of S'_1), each pair being isolated from other pairs, and the members of each pair being $O(\delta)$ apart. Denote $S_2 = \Lambda(S'_1) \cap S_1$; say there are M pieces. Each little piece of S_2 gets extended and folded under Λ to be inside S'_1 , and so there will be M folded ribbons the same shape as S'_1 inside S'_1 ; these constitute $S'_2 = \Lambda(S_2)$. Each folded ribbon of S'_2 gets mapped under Λ into S_2 and intersects each piece of S_2 . Denote $S_3 = \Lambda(S'_2) \cap S_2$; it consists of M^2 pieces. The pieces diminish in size geometrically with each iteration. By continuing this process, one can see that $S_\infty = \bigcap_1^\infty S_n$ is an invariant

set for Λ , and by construction has infinitely many periodic and aperiodic points. Basically, we are looking at a Smale horseshoe.

For different functions f , one could clearly have attracting chaotic behavior, as found for example by Marzec and Spiegel [12] and Baker et al. [1]. In this context, it is interesting to note that points on the strange invariant set can, to a certain extent, be characterized by a one-dimensional difference equation. Thus, if $(B, \theta) \in C_2$ and is on the invariant set, then we must have $\theta \approx 0$, so that

$$\begin{aligned} \theta' &\approx 2\pi N(B) \text{ mod } 2\pi \\ &= 2\pi N_f(B), \end{aligned} \tag{5.1}$$

say (N_f denotes fractional part). Thus (4.10)₂ is

$$B' = 1 - [1 - f(B)] g[|N_f(B)|'; B], \tag{5.2}$$

for $B \in P_3O$. The form of this map is shown in Figure 7 (cf. Figure 3). It is rather misleading, since it is unlikely that any of the points for which $N_f(B) = 0$ (i.e. for which there are cusps) will be on the invariant set, but its purpose is to compare it with a similar figure in [12] and to note that if f maps an interval into itself, then this cusped map is likely to be of relevance over its entire domain.

Finally we mention that, apart from the discussion in [19] at high r , there is some resemblance between the map Λ (see Figure 6) and the maps obtained numerically by Sparrow (although at much smaller values of r than are relevant here).

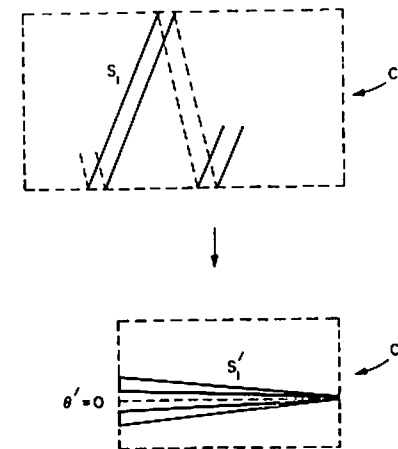


Figure 6. Plane views of S_1 and $S'_1 = \Lambda(S_1)$. Dimensions are highly exaggerated.

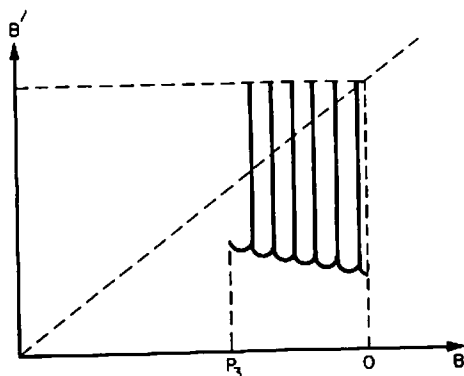


Figure 7. The mapping $B \rightarrow B'$ given by (5.2) (schematic).

References

1. N. H. BAKER, D. W. MOORE, and E. A. SPIEGEL, Aperiodic behavior of a nonlinear oscillator, *Quart. J. Mech. Appl. Math.* 24:391-422 (1971).
2. J. GRASMAN, H. NIJMEIER, and E. J. M. VELING, Singular perturbations and a mapping on the interval for the forced Van der Pol relaxation oscillator, Preprint, Mathematisch Centrum, Amsterdam, 1982.
3. P. HOLMES, A nonlinear oscillator with a strange attractor, *Philos. Trans. Roy. Soc. London Ser. A* A292:419-448 (1979).
4. P. J. HOLMES, Averaging and chaotic motions in forced oscillations, *SIAM J. Appl. Math.* 38:65-80 (1980).
5. L. N. HOWARD, Notes on the 1974 Summer Study Program in Geophysical Fluid Dynamics at WHOI, Woods Hole Oceanographic Institution, Woods Hole, Mass., 1974. This is the reference given in [16], although these notes are not contained in the 1974 Woods Hole GFD report. It is generally accepted that the scaling of the equations does originate with Howard, however (W. V. R. Malkus, private communication).
6. J. KEVORKIAN and J. D. COLE, *Perturbation Methods in Applied Mathematics*, Springer, Berlin, 1981.
7. S. KOGELMAN and J. B. KELLER, Asymptotic theory of nonlinear wave propagation, *SIAM J. Appl. Math.* 24:352-361 (1973).
8. G. E. KUZMAK, Asymptotic solutions of nonlinear second order differential equations with variable coefficients, *Prikl. Mat. Mekh.* 23:515-526; transl., *J. Appl. Math. Mech.* 23:730-744 (1959).
9. M. LEVI, Qualitative analysis of the periodically forced relaxation oscillations, *Mem. Amer. Math. Soc.*, Vol. 244, Amer. Math. Soc., Providence, R.I., 1981.
10. E. N. LORENZ, Deterministic nonperiodic flow, *J. Atmospheric Sci.* 20:130-141 (1963).
11. J. C. LUKE, A perturbation method for nonlinear dispersive wave problems, *Proc. Roy. Soc. London Ser. A* A292:403-412 (1966).
12. C. J. MARZEC and E. A. SPIEGEL, Ordinary differential equations with strange attractors, *SIAM J. Appl. Math.* 38:403-421 (1980).
13. J. P. POYET, Time-dependent convection, Ph.D. Thesis, Columbia University, New York, 1980.
14. M. RABINOVICH, Stochastic self-oscillations and turbulence, *Soviet Phys. Uspekhi* 21:443-469 (1978).
15. K. A. ROBBINS, Disk dynamos and magnetic reversal, Ph.D. Thesis, M.I.T., Cambridge, Mass., 1975.

16. K. A. ROBBINS, Periodic solutions and bifurcation structure at high R in the Lorenz model, *SIAM J. Appl. Math.* 36:457-472 (1979).
17. T. SHIMIZU, Analytic form of the simplest limit cycle in the Lorenz model, *Physica* 97A:383-398 (1979).
18. T. SHIMIZU and A. ICHIMURA, Asymptotic solution of a chaotic motion, *Phys. Lett. A* 91A:52-56 (1982).
19. C. SPARROW, The Lorenz equations: Bifurcations, chaos, and strange attractors, *Appl. Math. Sci.*, Vol. 41, Springer, Berlin, 1982.
20. V. I. YUDOVICH, Asymptotic behavior of limit cycles in the Lorenz system for large Rayleigh numbers, Thesis, Rostov State Univ., 1977.

MASSACHUSETTS INSTITUTE OF TECHNOLOGY

(Received September 16, 1983)